RSC Advances

This is an *Accepted Manuscript*, which has been through the Royal Society of Chemistry peer review process and has been accepted for publication.

Accepted Manuscripts are published online shortly after acceptance, before technical editing, formatting and proof reading. Using this free service, authors can make their results available to the community, in citable form, before we publish the edited article. This *Accepted Manuscript* will be replaced by the edited, formatted and paginated article as soon as this is available.

You can find more information about *Accepted Manuscripts* in the **Information for Authors**.

1 **Oxidative desulfurization of model fuel using ozone oxidation generated by**
2 **dielectric barrier discharge plasma combined with Co$_3$O$_4$/γ-Al$_2$O$_3$ catalysis**

3 **Cunhua Ma[1], Dong Chen[1], Fupeng Liu[1], Xishang Sun[1], Furong Xiao[1] and Bin Dai*[1]**

4 1 *School of Chemistry and Chemical Engineering, Shihezi University, Key Laboratory for Green Processing of*
5 *Chemical Engineering of Xinjiang Bintuan, Shihezi, Xinjiang 832003, PR China.*

6 * Corresponding author. Fax: +86 (0)993 2057270; Tel: +86 (0)993 2057277; *E-mail:* db_tea@shzu.edu.cn

7 **Abstract**

8   Oxidative desulfurization (ODS) method is highly promising method for deep desulfurization.

9 However, the oxidant used most often in ODS is hydrogen peroxide, which can decompose into

10 water and form an oil–water biphasic system, which affects fuel quality and confer difficulty in

11 recovering the oil phase. If a gas is used as an oxidizing agent in ODS, oil–water biphasic problems

12 would not exist. In this study, we synthesized metal oxide Co$_3$O$_4$/γ-Al$_2$O$_3$ as catalyst by

13 two-solvent, impregnation, and adsorption method, produced ozone as oxidant by the dielectric

14 barrier discharge (DBD) plasma technology, and prepared model fuel by dissolving representative

15 sulfur compounds such as thiophene (T), benzothiophene (BT), dibenzothiophene (DBT) and

16 4,6-dimethyldibenzothiophene (4,6-DMDBT) in n-octane. Then, a novel room temperature catalytic

17 oxidative desulfurization method through ozone oxidation combined with Co$_3$O$_4$/γ-Al$_2$O$_3$ catalysis

18 was developed. The method was suitable for the deep removal sulfur-containing compounds from

19 model fuel. This desulfurization technology efficiently removed T, BT, DBT, and 4,6-DMDBT, and

20 the sulfur removal of all sulfur compounds exceeded 99%.

21 **Keywords**

22 Oxidative desulfurization; Model fuel; DBD plasma; Ozone; Co$_3$O$_4$/γ-Al$_2$O$_3$

23

24

1. Introduction

Desulfurization from fuel oil is very important industrially. Fuel oil contains various kinds of sulfur compounds, such as thiol, sulfide, thiophene, benzothiophene, and its derivatives. Oil consumption accounted for more than 93% of total final energy consumed in the transportation sector.[1] Transportation fuels emit SO_x when they are burned. SO_x is a major source of air pollution and could damage human health,[2, 3] SO_x into the air can create acid rain, which corrodes buildings and destroys forests and crops.[4-7] As pollution worsens, people are becoming increasingly environmentally conscious and are paying an increasing amount of attention to the sulfur content in the oil in recent years. Governments worldwide are legislating stringent regulations to restrict sulfur concentration in transportation fuels to improve emission standards and reduce SO_x emissions.[8-14] Europe and America have been regulating the use of "sulfur-free" diesel and gasoline fuels ($\leq$10 ppm S) since 2009 and 2010, respectively.[15, 16] China had some disparities with the international convention and regulated that sulfur content in both gasoline and diesel was less than 50 ppm since 2010.[17, 18] Thus, lowering sulfur content and producing ultra-low sulfur fuels in China have been a difficult and challenging subject for researchers worldwide for quite some time.

Recently, compared to the conventional hydrodesulfurization (HDS), different types of non-hydrodesulfurization technologies, such as adsorptive desulfurization, extractive desulfurization, and ODS, have been significantly developed.[19-21] Although traditional HDS could effectively remove the majority of sulfur-containing compounds, this technique has several challenges, such as removing BT and its derivative, giving their larger steric hindrance. This difficult problem could be solved using the ODS method.[22] ODS technology is a process that converts organic sulfur into their related sulfone BTO and/or sulfoxide BTO_2 with stronger polarity than that of initial sulfur compounds and then removing it by extraction through strongly polar extractant according to the theory of "similarity and intermiscibility".[23] Some different types of oxidizers were used in ODS process, including hydrogen peroxide, ozone, molecular oxygen, and

1 organic peroxide. The DBD plasma has been often used to produce fresh ozone in the presence of

2 air or oxygen. Ozone is a very strong oxidant and easily oxidized the organic sulfur compounds.[24, 25]

3 ILs are a series of strong polar compounds solely consisted of organic cations and organic or

4 inorganic anions, so they can easier solvate and dissociate stronger polarity sulfone BTO and/or

5 sulfoxide BTO_2. Because of low vapor pressure, high thermal stability, easy to recycle, ILs received

6 significant attraction in green chemistry as a new green solvent, and have been applied in

7 desulfurization of fuel recently.[26-28]

8 Co_3O_4 has a normal spinel structure, and is by far the most frequently used in a wide range of

9 catalytic applications because it can be easily synthesized, as well as being chemically stable over a

10 wide range of temperatures and highly reactive at room temperature.[29, 30] Many factors significantly

11 affect catalytic activity and selectivity[31] of a supported catalyst in terms of dispersion of active

12 components, the interaction between the carrier and active components, and so on. These include

13 chemical nature, texture, and surface acidity of the support,[32] the composition of the metal

14 precursor,[33] the preparation method[34-36] and the metal loading,[37] etc. Activated aluminum oxide

15 γ-Al_2O_3 is a porous and highly dispersed solid material with a large surface area, and its porous

16 structure takes on an excellent adsorptive property, catalytic activity, and thermal stability.

17 Therefore, γ-Al_2O_3 can be widely used as catalyst carrier for preparing metal/metal oxide

18 nanoparticles.[38-41] Several synthetic methods for supported metal oxide catalysts are reported in the

19 literature. The conventional procedures are based on impregnation and adsorption. Recently a novel

20 method called a "two-solvent" technique for preparing metal oxide catalysts has attracted

21 considerable attention.[43] This method is reported to allow the preparation of highly dispersed metal

22 oxide nanoparticles.

23 In the present study, activated aluminum oxide γ-Al_2O_3 supported cobalt oxide Co_3O_4 using

24 $Co(NO_3)_2 \cdot 6H_2O$ as the precursor with various Co-content, which were prepared by the

25 impregnation, adsorption, and "two-solvent" technique. Then, the structures of prepared catalysts

1 were characterized using XRD, TEM and BET. The representative sulfur compounds such as T, BT,

2 DBT, and 4,6-DMDBT were chosen to prepare the model fuel. Moreover, catalytic ODS

3 performance of prepared catalysts were investigated using O_3 as oxidant combined with

4 [BMIM]CH_3COO ([BMIM]Ac) as the extractant at room temperature and pressure. A new

5 desulfurization technology was established by O_3 oxidation – catalysts catalysis – IL extraction.

6

7 **2. Experimental**

8 *2.1 Material and methods*

9   T, BT, DBT, 4,6-DMDBT, γ-Al_2O_3 and $Co(NO_3)_2·6H_2O$ were purchased from Aldrich/J&K

10 Chemical Ltd. IL, [BMIM]Ac were purchased from Lanzhou Zhongke Kaite Chemical New-tech

11 Co., Ltd.. They were used without any further treatment. Model fuel was prepared by dissolving T

12 (500 ppm sulfur content), BT (500 ppm sulfur content), DBT (100 or 500 ppm sulfur content) and

13 4,6-DMDBT (100 or 200 ppm sulfur content) in n-octane to provide model fuel.

14 *2.2 Co_3O_4/γ-Al_2O_3 catalysts preparation and characterization*

15   Supported cobalt oxide catalysts Co_3O_4/γ-Al_2O_3 were prepared using the two-solvent method

16 (TS), impregnation method (IM), and adsorption method (AD). The samples are recorded as Y-X-A,

17 where Y represents TS or IM or AD, X represents the nominal Co-loading percentage, and A

18 represents support γ-Al_2O_3. In all cases, $Co(NO_3)_2·6H_2O$ was used as the Co precursor. Detailed

19 preparation methods have been reported elsewhere.[39, 43, 44] All samples were dried at 100 °C

20 overnight, then calcined by heating in air at 2 °C·min^{-1} and holding at 500 °C for 6 h.

21   The structural properties of the prepared catalysts were characterized using various

22 characterization methods. The Co_3O_4 content was measured by inductively coupled plasma-atomic

23 emission spectrometry (ICP-AES) after digestion in HF/HNO_3, prior to measurement all catalysts

24 were digested with nitric acid and hydrofluoric acid. Wide-angle X-ray diffraction patterns were

1 obtained using a Bruker D8 Advance powder diffractometer (Bruker Company in Germany) in the

2 scan range of 2θ between 10 and 80˚ with a monochromatic Cu Kα source radiation at 40 kV and

3 40 mA. The data was collected with a step size of 0.02˚. N_2-adsorption/desorption isotherms were

4 determined using liquid nitrogen adsorption at approximately -196 °C by an ASAP 2020C surface

5 area and porosity analyzer (Micromeritics Instrument Corporation, USA). The samples were

6 outgassed at approximately 150 °C for 6 h before analysis. Pore volume, specific areas, and the pore

7 size distribution (PSD) (BJH method) were calculated using the BET equation. Transmission

8 electron microscopy (TEM) was used to obtain detailed information on the micro-morphology of

9 the Co_3O_4.

10 *2.3 Experimental apparatus of O_3 preparation and ODS process*

11 The schematic diagram of the experimental apparatus of O_3 preparation is shown in Fig. 1. The

12 whole setup consisted of a plasma power (CTP-2000K, Nanjing Suman electronic Co., Ltd), a DBD

13 reactor, a mass flow controller, a variable-voltage transformer, and an oscilloscope (RIGOL

14 DS1102E). And O_3 was prepared used a wire-cylinder reactor through self-assembly.

15 The wire-cylinder reactor is a quartz glass tube 2 mm thick. A 3 mm thick steel rod attached to

16 the AC high voltage (HV) electrode of plasma power is fixed in the axial center of reactor, and a

17 layer of steel net 70 mm in length attached to the AC low electrode (LV) of plasma power is

18 covered outside the reactor. The two electrodes are 4, 6 and 8 mm apart, respectively. Air is

19 generated using an air compressor, and then introduced into the DBD reactor with a mass flow

20 controller at a 100mL·min^{-1} flow rate. When the voltage applied to the two electrodes was 19.5 kV

21 (with a frequency value of 14.3 kHz) and is higher than the breakdown voltage of air, the air is

22 discharged by gas breakdown. Meanwhile, high-energy electrons and highly reactive oxygen-free

23 radicals are generated in the reactor. Then, excess oxygen reacts rapidly with oxygen-free radicals

24 to form fresh O_3. As an oxidant, the O_3 product from the bottom of reactor was introduced into

25 model oil to perform a desulfurization study. Ozone concentration was determined using

1   CJ/T3028.2–94 (the Chinese Standard). The process was conducted under normal atmospheric

2   pressure and temperature.

3   *2.4 Catalytic Oxidative desulfurization procedure*

4   Fig. 1 shows that the catalytic oxidative desulfurization experiment was conducted in a 10 mL

5   two-necked flask. At room temperature, a certain amount of model oil and $Co_3O_4/\gamma-Al_2O_3$ catalyst

6   was added into flask, and then the prepared O_3 was fed into the mixture to oxidize sulfur

7   compounds with a reflux condenser under magnetic stirring. After oxidation for a definite time, a

8   certain quantity of IL [BMIM]Ac was used for an extraction experiment under a magnetic stirrer at

9   room temperature. According to the desired extraction time, the supernatant oil phase was

10   periodically taken after thorough standing, and the sulfur content was analyzed by microcoulometry

11   (WK-2D, Jiangsu Jiangfen Electroanalytical Instrument Co., Ltd., China).

12   **3. Results and Discussion**

13   *3.1 Characterization of $Co_3O_4/\gamma-Al_2O_3$ catalysts*

14   The Co_3O_4 content of the prepared catalysts are summarized in Table 1. The Co_3O_4 content

15   differed from preparation methods to preparation methods. The actual Co_3O_4 contents of IM-5%-A

16   and TS-5%-A were closer to the nominal loading. However, the catalyst AD-5%-A showed lower

17   Co_3O_4 content due to weak interactions between the $\gamma-Al_2O_3$ support and the cobalt precursor. The

18   actual loading amount of Co_3O_4 in catalyst IM-5%-A before and after ODS had almost equal weight,

19   demonstrating the superior stability of the $Co_3O_4/\gamma-Al_2O_3$ catalyst.

20   Fig. 2 shows the wide-angle XRD patterns of $\gamma-Al_2O_3$ supporter, Co_3O_4 and $Co_3O_4/\gamma-Al_2O_3$

21   catalysts prepared through equal volume impregnation at various Co-loadings. The results showed

22   that all Co-loading materials had the same crystal structures, and the main diffraction peaks

23   matched exactly with the standard card of Co_3O_4 (JCPDS 78-1970) with almost the same peak

24   resolution. Thus, the prepared samples exhibited a pure Co_3O_4 crystalline phase. When the loading

1 amount of Co_3O_4 was 2.5% (mass percentage)，the spinel structure of Co_3O_4 was obvious. The

2 intensity of the diffraction peak of γ-Al_2O_3 decreased and the peak width broadened after

3 Co-loading, which could be attributed to superposition of the characteristic peak of γ-Al_2O_3 and

4 Co_3O_4, such as 2θ = 66°. Moreover, the intensity of the diffraction peak of Co_3O_4 sharpened, which

5 could be attributed to reduction in the extent of the γ-Al_2O_3, such as 2θ = 36.978°.Co_3O_4 had a

6 highly preferred orientation to the (311) face.

7 Fig. 3 gives the XRD patterns of Co_3O_4/γ-Al_2O_3 catalysts prepared through different methods

8 at 5 wt% Co-loading. Some characteristic peaks of Co_3O_4 in the TS-5%-A and AD-5%-A catalysts

9 were not obvious compared with Co_3O_4 in IM-5%-A; both catalysts had two weak peaks at 2θ =

10 31.38° and 2θ = 59.58°. Moreover, some essential characteristic peaks were not detected. Which

11 could be attributed to the following reasons: (1) Base on the TEM image, the active components

12 Co_3O_4 prepared using TS was dispersed in the channels of the mesoporous γ-Al_2O_3; and (2) the

13 actual loading amount of active components Co_3O_4 prepared by AD was less than that by TS and

14 IM according to Table 1.

15 The textural parameters of γ-Al_2O_3 and all the Co-composites synthesized by IM, including

16 BET surface area, total pore volume and average pore size, are summarized in Table 1. Compared

17 with pure γ-Al_2O_3, the surface area of all the Co-composites showed a significant decreasing trend

18 as Co_3O_4 loading increased. When Co_3O_4 loading was only 2.5 wt%, the surface area declined very

19 slightly (from 182.0 m^2/g to 178.4 m^2/g); but when Co_3O_4 loading increased to 15 wt%, the surface

20 area dropped to 106.24 m^2/g rapidly. The active ingredient Co_3O_4 deposited on the surface of the

21 supporter is the major reason for the falling surface. The average pore size of all the Co-composites

22 slightly decreased as Co_3O_4 loading increased, which indicates that the active components of Co_3O_4

23 were well dispersed in the channels and on the surfaces of the carrier.

24 Fig. 4 shows the N_2 adsorption-desorption isotherms of the γ-Al_2O_3 and all the Co-composites

25 prepared using different methods. All the samples showed type IV isotherms with H3-type

1   hysteresis loops according to the IUPAC classification, which is typical for mesoporous materials.

2   Fig. 4 shows that all the samples presented isotherms with identical shapes to that of γ-Al$_2$O$_3$ after

3   Co$_3$O$_4$ was loaded, which is indicative of the preservation of the mesoporous structure for relatively

4   low Co-loadings. However, the volume of adsorbed N$_2$ decreased as Co-loading increased.

5   Moreover the capillary condensation region shifted to a lower relative pressure compared to pure

6   γ-Al$_2$O$_3$. These changes, together with reduction in the surface areas and pore volume of the

7   Co-composites, were ascribed to the blockage of channel by cobalt species (Table 1).

8   The pore size distribution of γ-Al$_2$O$_3$, Co$_3$O$_4$ and Co-composites are shown in Fig. 5. The

9   results show that Co$_3$O$_4$ can be regarded as a solid with little pore. The pore structure of AD-5%-A

10   had no significant differences compared to pure γ-Al$_2$O$_3$, but the center of the peak slightly shifted

11   to a lower pore width for TS-5%-A and IM-5%-A. Thus, the average pore size decreased after the

12   formation of Co$_3$O$_4$ inside the pores of the carrier. This result demonstrated that Co$_3$O$_4$ was easier to

13   deposit on the surface of the support prepared by TS and IM. From the pore volume and surface

14   area, Co$_3$O$_4$ was easier to enter into the pores of the support prepared using TS. In comparison to

15   IM-5%-A, the centre of the peak of the sample IM-15%-A shifted to a lower pore width, illustrated

16   that more Co$_3$O$_4$ particles blocked the pores of the support.

17   Fig. 6 provides the TEM images of the catalysts IM-5%-A, TS-5%-A and the support γ-Al$_2$O$_3$.

18   For the catalysts IM-5%-A and TS-5%-A, the ordered hexagonal channels in the mesoporous Al$_2$O$_3$

19   were preserved after cobalt loading. This result was consistent with that obtained by XRD. Large

20   patches were clearly observed on IM-5%-A catalyst, showing that Co$_3$O$_4$ aggregation occurred. The

21   patches diameter was larger than channels diameter of the support γ-Al$_2$O$_3$. No aggregated particles

22   were found on TS-5%-A, showing that Co$_3$O$_4$ was highly dispersed in the channels of the

23   mesoporous γ-Al$_2$O$_3$.

24   *3.2 Effect of the electrode distance between the two electrodes on ozone concentration*

25   When discharge voltage is 19.5 kV, and the air flow rate is 100 mL·min^{-1}, The ozone

1   generation rate histogram is shown in Fig. 7, in which the electrode distance between the two

2   electrodes is 4mm, 6 mm and 8 mm apart, respectively. It can be seen from Fig. 7 that the electrode

3   distance had a tremendous influence on ozone concentration. When the electrode distance between

4   the two electrodes was shortened twice, the ozone concentration increased approximately 5 times.

5   When the electrode distance was 8 mm, the ozone concentration was 1.31 mg·L^{-1}. When the

6   electrode distance was 4 mm, the ozone concentration was 5.48 mg·L^{-1}. With the decreasing

7   discharge distance, the amount of ozone increased because the probability of efficient collision was

8   enhanced between the high-energy electrons generated by DBD and oxygen in a more narrow

9   discharge space for the formation of more ozone. Later research found that the mount of ozone met

10   the requirements of oxidative desulfurization experiments with a discharge distance of 8 mm. Thus,

11   an electrode distance of 8 mm was selected for use in the late-stage ODS study.

12   *3.3 Catalytic ODS test of Co_3O_4/γ-Al_2O_3*

13   *3.3.1 Desulfurization comparisons at different desulfurization system of Co_3O_4/γ-Al_2O_3*

14   In the hydrodesulfurization process, generally DBT was chosen as the representative sulfur

15   compound in fuels. Therefore, model fuel with a sulfur content of 100 ppm that contains DBT were

16   conducted to study the following catalytic ODS experiments. To evaluate the catalytic activities of

17   Co_3O_4/γ-Al_2O_3 catalyst in different desulfurization systems (Table 2), we selected 0.05 g

18   IM-10%-A as a catalyst and reacted for 30 min to investigate the desulfurization of different

19   catalytic systems. Furthermore, the result was compared with the desulfurization activity of pure O_3

20   or pure γ-Al_2O_3. The results are listed in Table 2.

21   From the data listed in Table 2, it can be seen that IM-10%-A catalyst removed DBT with a

22   sulfur content of 100 ppm from the model fuel entirely when O_3 was used as oxidant. However,

23   sulfur removal was only 43.3% when O_2 was used as an oxidant. This result revealed that the

24   oxidizability of O_2 on DBT was far less than that of O_3 used the same catalyst under identical

1 experimental conditions. In addition, if IM-10%-A or γ-Al$_2$O$_3$ was directly used for desulfurization

2 without any oxidizing agent added, the DBT removal could reach approximately 35%. At this point,

3 desulfurization method was turned into adsorption desulfurization. Compared to the ODS by O$_2$,

4 DBT removal had no significant differences, which further illustrated the weak oxidizing capacity

5 of O$_2$ on DBT. Table 3 also shows that DBT was hardly oxidized by O$_3$ without Co$_3$O$_4$/γ-Al$_2$O$_3$

6 existences.

7 *3.3.2 Effect of the catalyst loading amount on DBT removal*

8   The effect of the catalyst loading amount on DBT removal was investigated. The result is

9 indicated in Fig. 8. As shown in Fig. 8, the desulfurization rate obviously increased with increasing

10 amount of Co-loading. When DBT was oxidized for approximately 5 min, the DBT removal of

11 IM-15-A exceeded 60%. When increased oxidative time was 20 min，the DBT removal of four

12 different Co-loading catalysts reached over 95%, and IM-12.5-A and IM-15-A were 99.9%. When

13 O$_3$ used to oxidize DBT for 30 min, the desulfurization rate of all Co$_3$O$_4$/γ-Al$_2$O$_3$ catalysts with

14 different supported Co$_3$O$_4$ content reached 99.9%. From Fig. 8, the amount of Co-loading had a

15 remarkable effect on DBT removal when oxidation time was less than 10 min. However, the

16 amount of Co-loading had no obvious difference on DBT removal when oxidation time was more

17 than 20 min.

18 *3.3.3 Desulfurization comparisons of Co$_3$O$_4$/γ-Al$_2$O$_3$ prepared by different methods on DBT*

19 *removal*

20   At the same ODS condition, the catalytic activity of Co$_3$O$_4$/γ-Al$_2$O$_3$ at 5% loading prepared by

21 IM, TS, and AD was researched. The results are shown in Fig. 9. The catalytic performance of three

22 Co$_3$O$_4$/γ-Al$_2$O$_3$ catalysts rapidly increased with the extension of oxidation time and the sulfur

23 removal all reached 99.9% at 30 min oxidization with O$_3$. Moreover, TS-5%-A had excellent

24 catalytic activity and a desulfurization efficiency of 95% was obtained after oxidizing for 5 min,

1   illustrated Co_3O_4 particles diffused into the holes of γ-Al_2O_3. The result agrees with the discussion

2   regarding pore-size distribution (Fig. 5) and TEM (Fig. 6).

3   *3.3.4 The influence of O_3 concentration on DBT removal*

4   The influence of O_3 concentration on DBT removal was investigated, and the result is

5   indicated in Fig. 10. In the preceding work of our project group,[45] the consistence of O_3 could

6   be adjusted by adjusting air flow rate, and increased with the decrease of the air flow rate. As shown

7   in Fig. 10, the O_3 concentration had remarkable effects on DBT removal. Only 93.8% DBT removal

8   was reached when 0.71 mg·L^{-1} O_3 was bubbled into the oxidation system. However, the

9   desulfurization rate of DBT increased to 99.5% as the O_3 concentration increased to 1.19 mg·L^{-1}.

10   As the O_3 concentration was set to 1.31 mg·L^{-1} [Air flow rate = 100 mL·min^{-1}], approximately

11   99.9% DBT removal was reached.

12   *3.3.5 Desulfurization comparisons of different sulfur compounds by Co_3O_4/γ-Al_2O_3*

13   In terms of its advantageous catalytic reaction performance, IM-15-A was selected as the most

14   ideal for studying the effect of different substrates such as TS, BT, DBT, and 4, 6-DMDBT on ODS

15   in the O_3 – Co_3O_4/γ-Al_2O_3 – [BMIM]Ac system under the same experimental conditions. Table 4

16   exhibits that IM-15-A had excellent catalytic activity to four sulfur-containing compounds. For 500

17   ppm T and BT, 100 DBT ppm and 4,6-DMDBT, and 200 ppm 4,6-DMDBT, the desulfurizing ratio

18   reached to above 99.6%. However, for 500 ppm DBT，the desulfurizing ratio decreased to 93.1%.

19   *3.3.6 Reusability of the catalyst Co_3O_4/γ-Al_2O_3*

20   The recyclability of the IM-15%-A catalyst was evaluated and the results are shown in Fig. 11.

21   After the catalyst was oxidized, recovered by decantation, washed several times with methanol, and

22   subsequently dried at 100 ∘C. Then the fresh model oil and O_3 were introduced for the next recycle

23   under the same conditions. The data in Fig. 11 indicate that the catalyst was used up to five times

1   without significant change in its catalytic activity.

2   **4. Conclusions**

3   In this study, we synthesized metal oxide catalysts $Co_3O_4/\gamma-Al_2O_3$, and the Co_3O_4 was

4   accommodated inside the pores by the TS method. Moreover IL [BMIM]Ac was screened as an

5   extracting agent and the model fuel was prepared using representative sulfur compounds such as T,

6   BT, DBT, and 4,6-DMDBT in fuel oil. Then, the catalytic oxidation activities of prepared catalysts

7   and extracting performance of screened IL for model fuel desulfurization were studied using ozone

8   as an oxidant at room temperature and pressure. New desulfurization technology was established

9   through O_3 oxidation – catalysts catalysis – IL extraction. The results indicated that the oxidative

10   desulfurization technology using O_3 as oxidant in the presence of catalysts combined with IL

11   extraction was very effective, and TS-5%-A had excellent catalytic activity. Moreover, the sulfur

12   removal of T, BT, DBT, and 4,6-DMDBT all reached over 99% at ordinary temperatures and

13   pressures, respectively. In addition, the oxidation step was the key step in the desulfurization

14   process. Desulfurization was lower or ineffective if T, BT, DBT, or 4,6-DMDBT was not oxidized

15   to the corresponding oxidization product. The IM-15%-A catalyst can be used repeatedly 5 times,

16   and its catalytic activity was no significant change.

17   **Acknowledgements**

22   **References**

1   [1]   M. Keshavarzian, S. Kamali Anaraki, M. Zamani and A. Erfanifard, *Econ. Model.*, 2012, **29**,

2   1979–1985.

3   [2]   A. Aguiar, S. Ribeiro, A. Silva, L. Cunha-Silva, B. de Castro, A. M. Silva and S. S. Balula,

4   *Appl. Catal.*, *A*, 2014, **478**, 267–274.

5   [3]   X. D. Qiang, F. Fu, D. J. Wang and L. Guo, *Adv. Mater. Res.*, 2012, **518**, 750–754.

6   [4]   R. T. Yang, A. J. Hernandez-Maldonado and F. H. Yang, *Science*, 2003, **301**, 79–81.

7   [5]   F. Al-Shahrani, T. Xiao, S. A. Llewellyn, S. Barri, Z. Jiang, H. Shi and M. L. Green, *Appl.*

8   *Catal.*, *B*, 2007, **73**, 311–316.

9   [6]   G. Yu, J. Zhao, D. Song, C. Asumana, X. Zhang and X. Chen, *Ind. Eng. Chem. Res.*, 2011,

10   **50**, 11690–11697.

11   [7]   C. Asumana, G. Yu, X. Li, J. Zhao, G. Liu and X. Chen, *Green Chem.*, 2010, **12**, 2030–2037.

12   [8]   L. Ban, P. Liu, C. Ma and B. Dai, *Catal. Today*, 2013, **211**, 78–83.

13   [9]   C. Sentorun-Shalaby, S. K. Saha, X. Ma and C. Song, *Appl. Catal.*, *B*, 2011, **101**, 718–726.

14   [10]   S. Xun, W. Zhu, D. Zheng, H. Li, W. Jiang, M. Zhang, Y. Qin, Z. Zhao and H. Li, *RSC Adv.*,

15   2015, **5**, 43528-43536.

16   [11]   E. Lissner, W. F. de Souza, B. Ferrera and J. Dupont, *ChemSusChem*, 2009, **2**, 962–964.

17   [12]   H. Gao, S. Zeng, X. Liu, Y. Nie, X. Zhang and S. Zhang, *RSC Adv.*, 2015, **5**, 30234-30238.

18   [13]   P. S. Kulkarni and C. A. M. Afonso, *Green Chem.*, 2010,**12**, 1139–1149.

19   [14]   W. Zhu, J. Zhang, H. Li, Y. Chao, W. Jiang, S. Yin and H. Liu, *RSC Adv.*, 2012, **2**, 658-664.

20   [15]   O. Kröcher, M. Widmer, M. Elsener and D. Rothe, *Ind. Eng. Chem. Res.*, 2009, **48**,

21   9847–9857.

22   [16]   L. Lu, S. Cheng, J. Gao, G. Gao and M. Y. He, *Energ. Fuel*, **21**(2007) 383–384.

23   [17]   GB 19147-2013. *Automobile diesel fuels (V)* [S], China, 2013.

24   [18]   GB 17930-2011. *Gasoline for motor vehicles* [S], China, 2011.

25   [19]   V. C. Srivastava, *Rsc Adv.,* 2012, 2, 759-783.

1   [20]   L. Ban, P. Liu, C. Ma and B. Dai, *Chinese Chem. Lett*., 2013, **24**, 755–758.

2   [21]   R. Abro, A. A. Abdeltawab, S. S. Al-Deyab, G. Yu, A. B. Qazi, S. Gao, and X. Chen, *RSC*

3   *Adv*., 2014, **4**, 35302-35317.

4   [22]   H. Li, X. Jiang, W. Zhu, J. Lu, H. Shu and Y. Yan, *Ind. Eng. Chem. Res*., 2009, **48**,

5   9034–9039.

6   [23]   C. Ma, B. Dai, C. Xu, P.Liu, L. Qi and L. Ban, *Catal. Today*, 2013, **211**, 84–89.

7   [24]   N. Mastanaiah, P. Banerjee, J. A. Johnson and S. Roy, *Plasma Process Polym*., 2013, **10**,

8   1120–1133.

9   [25]   D. Kuvshinov, A. Siswanto, J. Lozano-Parada and W. B. Zimmerman, *World Acad. Sci. Eng.*

10   *Technol*., 2014, **8**, 80–83.

11   [26]   B. Rodríguez-Cabo, H. Rodríguez, E. Rodil, A. Arce and A. Soto, *Fuel*, 2014, **117**, 882–889.

12   [27]   X. Chen, S. Yuan, A. A. Abdeltawab, S. S. Al-Deyab, J. Zhang, L.Yu and G. Yu, *Sep. Purif.*

13   *Technol.*, 2014, **133**, 187–193.

14   [28]   S. A. Dharaskar, K. L.Wasewar, M. N.Varma, D. Z. Shende and C. K. Yoo, *Ind. Eng. Chem.*

15   *Res*, 2014, **53**, 19845–19854.

16   [29]   P. H. Shi, H. G. Zheng, W. F. Yao, Q. Wu, S. Y. Tan and H. J. Pang, *Adv. Mater. Res.*, 2014

17   955, 62–65.

18   [30]   J. Taghavimoghaddam, G. P. Knowles and A. L. Chaffee, *J. Mol. Catal.*, *A*, 2012, **358**, 79–88.

19   [31]   D. Yin, W. Li, W. Yang, H. Xiang, Y. Sun, B. Zhong and S. Peng, *Micropor. Mesopor. Mater*.,

20   2001, **47**, 15–24.

21   [32]   A. Y. Khodakov, R. Bechara and A. Griboval-Constant, *Appl. Catal.*, *A*, 2003, **254**, 273–288.

22   [33]   T. Vralstad, G. Øye, M. Rønning, W. R. Glomm, M. Stocker and J. Sjoblom, *Micropor.*

23   *Mesopor. Mater*., 2005, **80**, 291–300.

24   [34]   G. Laugel, J. Arichi, M. Moliere, A. Kiennemann, F. Garin and B. Louis, *Catal. Today*, 2008,

25   **138**, 38–42.

1   [35]   L. Jiao and J. R. Regalbuto, *J. Catal.*, 2008, **260**, 342–350.

2   [36]   C. Wang, S. Lim, G. Du, C. Z. Loebicki, N. Li, S. Derrouiche and G. L. Haller, *J. Phys. Chem.*

3   *C*, 2009, **113**, 14863–14871.

4   [37]   J. Panpranot, J. G. Goodwin and A. Sayari, *Catal. Today*, 2002, **77**, 269–284.

5   [38]   J. H. Kwak, J. Hu, D. Mei, C. W. Yi, D. H. Kim, C. H. Peden and J. Szanyi, *Science*, 2009,

6   **325**, 1670–1673.

7   [39]   R. Zhang, B. Wang, H. Liu and L. Ling, *J. Phys. Chem. C*, 2011, **115**, 19811–19818.

8   [40]   C. Gu, J. Miao, Y. Liu and Y. Wang, *J. Mater Sci.*, 2010, **45**, 5660–5668.

9   [41]   X. P. Auvray and L. Olsson, *Catal. Lett.*, 2014, **144**, 22–31.

10 [42]   M. Imperor-Clerc, D. Bazin, M. D. Appay, P. Beaunier and A. Davidson, *Chem. Mater.*, 2004,

11   **16**, 1813–1821.

12 [43]   J. Taghavimoghaddam, G. P. Knowles and A. L. Chaffee, *Top. Catal.*, 2012, **55**, 571–579.

13 [44]   J. Taghavimoghaddam, G. P. Knowles and A. L. Chaffee, *J. Mol. Catal.*, *A*, 2013, 377,

14   115–122.

15 [45]   C. Ma, B. Dai, P. Liu, N. Zhou, A. Shi, L. Ban and H. Chen, *J. Ind. Eng. Chem.*, 2014, **20**,

16   2769–2774.

17

18

19

20

21

22

23

24

25

1   **Figure Captions page**

2

3   **Fig. 1**   The schematic of the experimental apparatus of O_3 preparation and ODS process

4   **Fig. 2**   XRD patterns of Co_3O_4/γ-Al_2O_3 catalysts by IM

5   **Fig. 3**   XRD patterns of Co_3O_4/γ-Al_2O_3 catalysts by IM, TS and AD

6   **Fig. 4** N_2 adsorption-desorption isotherms of γ-Al_2O_3 and Co-composites

7   **Fig. 5**   Pore size distribution of γ-Al_2O_3, Co_3O_4 and Co-composites

8   **Fig. 6**   The TEM images of samples: (A) IM-5%-A; (B) TS-5%-A; (C) Al_2O_3

9   **Fig. 7**   Effect of the electrode distance between the two electrodes on O_3 concentration

10   **Fig. 8**   Effect of Co_3O_4 loading on γ-Al_2O_3 on DBT removal

11   **Fig. 9**   Effect of preparation method of Co_3O_4/γ-Al_2O_3 catalyst on DBT removal

12   **Fig. 10**   Effect of O_3 concentration of DBT removal

13   **Fig. 11**   Reusability of IM-15%-A for DBT removal

14

15   **Table 1**   The actual content of Co_3O_4 in Co_3O_4/γ-Al_2O_3

16   **Table 2**   Surface area, average pore size and pore volume of samples

17   **Table 3**   Desulfurization comparisons at different desulfurization system of Co_3O_4/γ-Al_2O_3

18   **Table 4**   T, BT, DBT and DMDBT removal by Co_3O_4/γ-Al_2O_3

19
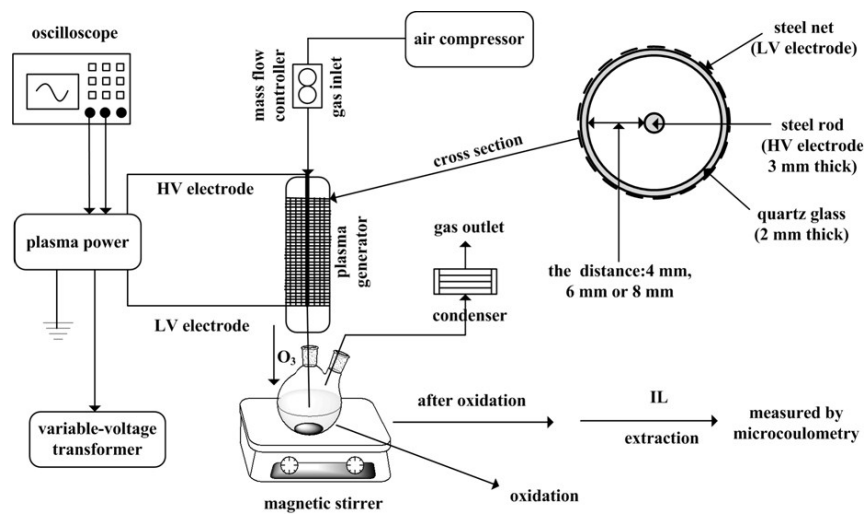
Fig. 1   The schematic of the experimental apparatus of O_3 preparation and ODS process
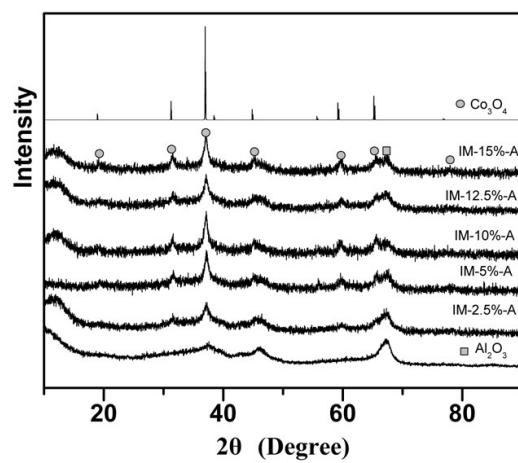
Fig. 2   XRD patterns of Co_3O_4/γ-Al_2O_3 catalysts by IM
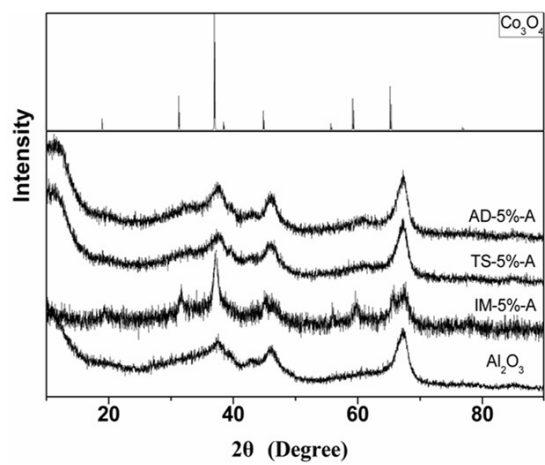
Fig. 3 XRD patterns of Co_3O_4/γ-Al_2O_3 catalysts by IM, TS and AD
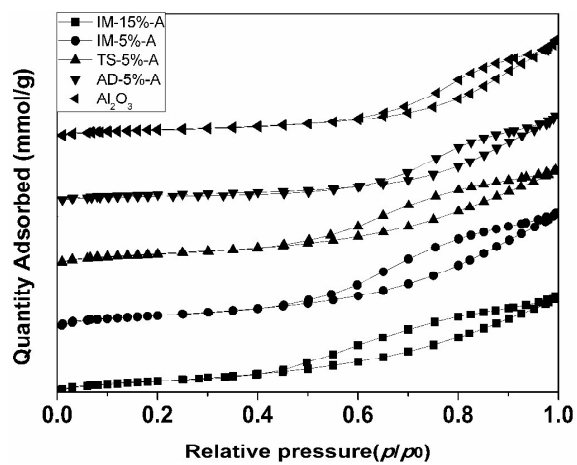
Fig. 4 N$_2$ adsorption-desorption isotherms of γ-Al$_2$O$_3$ and Co-composites
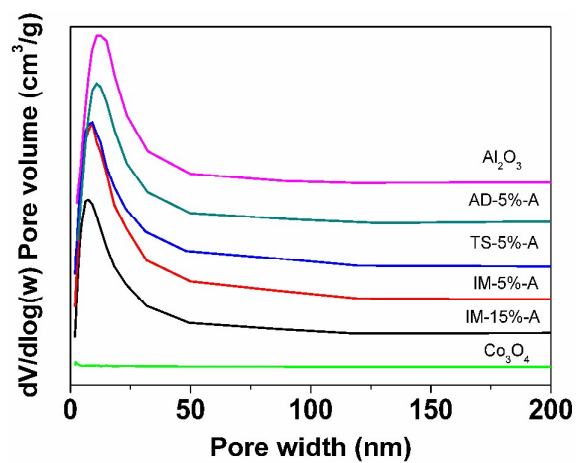
Fig. 5 Pore size distribution of γ-Al_2O_3, Co_3O_4 and Co-composites
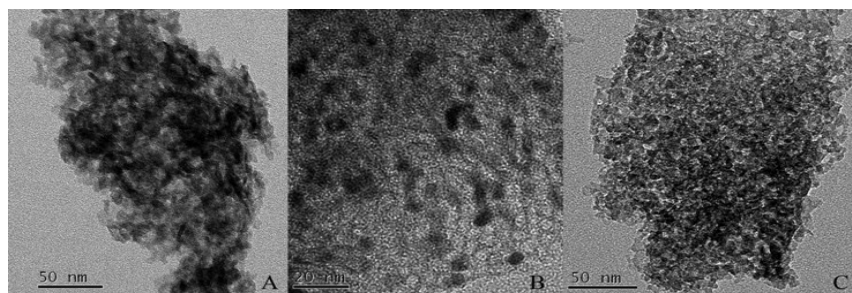
Fig. 6. The TEM images of samples: (A) IM-5%-A; (B) TS-5%-A; (C) Al_2O_3
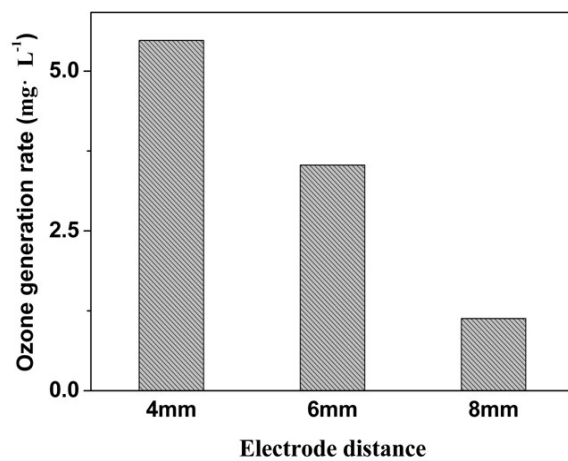
Fig. 7   Effect of the electrode distance between the two electrodes on O_3 concentration
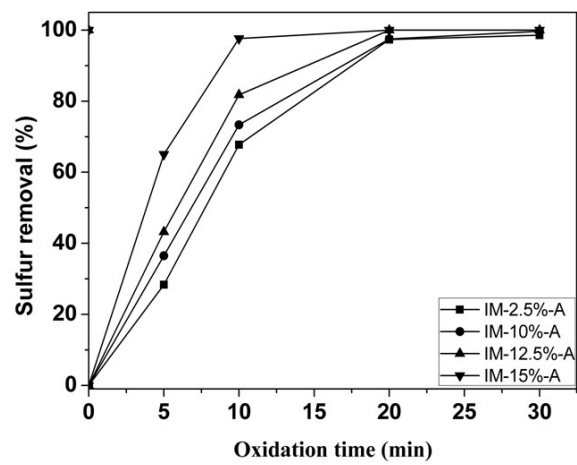
Fig. 8 Effect of Co_3O_4 loading on γ-Al_2O_3 on DBT removal
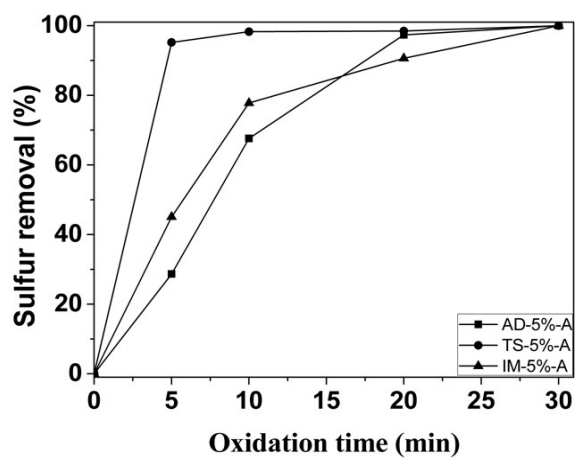
Fig. 9 Effect of preparation method of Co_3O_4/γ-Al_2O_3 catalyst on DBT removal
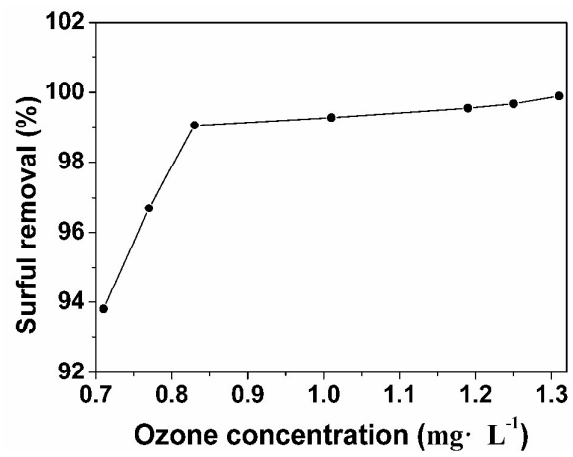
Fig. 10   Effect of O_3 concentration of DBT removal
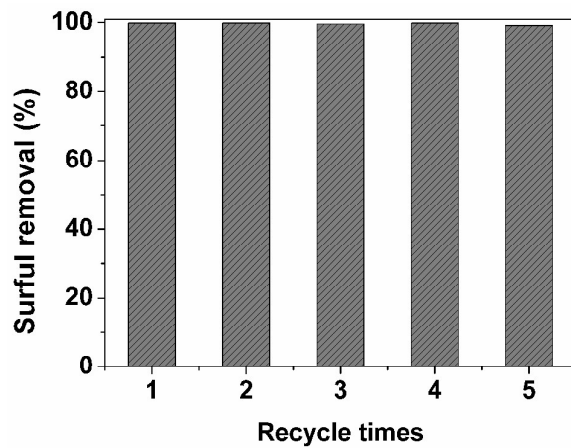
Fig. 11   Reusability of IM-15%-A for DBT removal

Table 1   The actual content of Co_3O_4 in $Co_3O_4/\gamma\text{-}Al_2O_3$

Samples	Nominal Co_3O_4 content (wt%)	Actual Co_3O_4 content (wt%)
AD-5%-A	5	2.03
TS-5%-A	5	4. 03
IM-5%-A	5	4.26
IM-5%-A (After ODS)	5	4.11

Table 2 Surface area, average pore size and pore volume of samples

Samples	Surface area (m^2/g)	Pore volume (cm^3/g)	Average pore size (nm)
Al$_2$O$_3$	182.0	0.432	9.503
IM-2.5%-A	178.4	0.376	9.302
IM-5%-A	168.3	0.366	9.674
TS-5%-A	175.4	0.385	9.629
AD-5%-A	178.9	0.410	9.417
IM-10%-A	156.71	0.361	9.218
IM-12.5%-A	144.21	0.331	9.194
IM-15%-A	106.24	0.255	9.105

Table 3   Desulfurization comparisons at different desulfurization system of $Co_3O_4/\gamma\text{-}Al_2O_3$

	Co_3O_4/Al_2O_3	Sulfur-removal (%)
（1）	IM-10%-A + O_3	99.9
（2）	IM-10%-A + O_2	43.3
（3）	IM-10%-A	36.14
（4）	O_3	2.0
（5）	Al_2O_3	35.13

Table 4   T, BT, DBT and DMDBT removal by Co_3O_4/γ-Al_2O_3

Model fuel	Initial S-concentration (ppm)	Sulfur removal (%)
T	500	99.9
BT	500	99.6
DBT	100	99.9
	500	93.1
4,6-DMDBT	100	99.9
	200	99.7